Intercomparison of Recent Anomaly Time-series of OLR as Observed by CERES and Computed using AIRS Products

Joel Susskind, NASA Goddard Space Flight Center[1]
Gyula Molnar, University Maryland University County[2]
Lena Iredell, Science Applications International Corporation[3]
Norman G. Loeb, NASA Langley Research Center[4]

[1]J. Susskind, NASA GSFC, Code 613, Greenbelt, MD 20771, Joel.Susskind-1@nasa.gov,
[2]G. Molnar, UMBC, NASA, Code 613, Greenbelt, MD 20771, Gyula.I.Molnar@nasa.gov,
[3]L. Iredell, SAIC, NASA, Code 613, Greenbelt, MD 20771, Lena.Iredell@nasa.gov,
[4]N. Loeb, NASA LARC, Mail Stop 420, Hampton, VA 23681, Norman.G.Loeb@nasa.gov

Abstract

This paper compares recent spatial and temporal anomaly time series of OLR as observed by CERES and computed based on AIRS retrieved surface and atmospheric geophysical parameters over the 7½ year time period September 2002 through February 2010. This time period is marked by a substantial decrease of OLR, on the order of −0.1 W/m^2/yr, averaged over the globe, and very large spatial variations of changes in OLR in the tropics, with local values ranging from −2.8 W/m^2/yr to +3.1 W/m^2/yr. Global and Tropical OLR both began to decrease significantly at the onset of a strong La Niña in mid-2007. Late 2009 is characterized by a strong El Niño, with a corresponding change in sign of both Tropical and Global OLR anomalies. The spatial patterns of the 7½ year short term changes in AIRS and CERES OLR have a spatial correlation of 0.97 and slopes of the linear least squares fits of anomaly time series averaged over different spatial regions agree on the order of ±0.01 W/m^2/yr. This essentially perfect agreement of OLR anomaly time series derived from observations by two different instruments, determined in totally independent and different manners, implies that both sets of results must be highly stable. This agreement also validates the anomaly time series of the AIRS derived products used to compute OLR and furthermore indicates that anomaly time series of AIRS derived products can be used to explain the factors contributing to anomaly time series of OLR.

1. Introduction

OLR (Outgoing Longwave Radiation) represents the total radiation going to space emitted by the earth-atmosphere system. OLR, a critical component of the earth's radiation budget has been measured globally since 1975 by the ERB instrument on the Nimbus-6 and Nimbus-7 satellites (Jacobowitz et al., 1984, Kyle et al., 1993), the ERBE instrument on NOAA-9, NOAA-10 and ERBS (Barkstrom 1989), the AVHRR instrument on NOAA operational satellites (Gruber et al., 1994 and references therein) and most recently by CERES which has flown on EOS Terra since 2000 and Aqua (Wielicki et al., 1996).

OLR has been widely used as a proxy for convective activity and rainfall, particularly in diagnosing and understanding tropical intraseasonal to interannual variability and monsoons (e.g. Chiodi and Harrison 2010, Kidson et al. 2002, Hoyos and Webster 2007, Barlow et al. 2005, Kiladis et al. 2005, Jones et al., 2004). In addition, OLR has been used in studies of earth's radiation balance (e.g. Fasullo and Trenberth, 2008) and atmospheric model validation (e.g. Allan et al., 2003). More importantly, anomalies and trends of OLR have been used to study climate feedbacks and processes (e.g. Chung et al. 2010, Huang and Ramaswamy 2009, Soden and Held 2006, Chu and Wang, 1997).

OLR at a given location is affected primarily by the earth's surface temperature; atmospheric vertical temperature and water vapor profiles; and the heights and amounts of multiple layers of cloud cover. OLR also depends on the vertical distribution of trace gases such as O_3, CH_4, CO_2, and CO. OLR can be computed for a given Field of Regard (FOR), given all the needed geophysical parameters, by use of an OLR

Radiative Transfer Algorithm (RTA). Mehta and Susskind developed such an OLR RTA and applied it to products observed by TOVS (TIROS Operational Vertical Sounder) derived using the TOVS Path-A Pathfinder retrieval methodology (Susskind et al., 1997) in order to generate the TOVS Pathfinder Path-A OLR data set (Mehta and Susskind 1999a, 1999b).

Mehta and Susskind compute OLR, referred to as F below, as a sum of 14 spectral components according to the equation

$$F = \sum_{j=1}^{14} F_j = \sum_{j=1}^{14} (1 - \alpha\varepsilon_{1j} - \alpha\varepsilon_{2j}) F_{j,CLR} + \alpha\varepsilon_{1j} F_{j,CLD1} + \alpha\varepsilon_{2j} F_{j,CLD2} \qquad (1)$$

where $F_{j,CLR}$ is the computed clear sky flux going to space integrated over all angles, emanating from spectral band j; $F_{j,CLDk}$ is the analogous flux emanating from an opaque cloud at cloud top pressure p_k; and $\alpha\varepsilon_{kj}$ is the radiatively effective cloud fraction which is the product of the geometric fractional cloud cover α_k for the cloud at pressure p_k as seen from above and ε_{kj}, the emissivity of that cloud in spectral interval j. Mehta and Susskind parameterize F_j as a function of surface skin temperature, surface spectral emissivity in spectral band j, ε_j, and atmospheric temperature, water vapor, and ozone profiles. The parameterizations are done based on line-by-line calculations (Susskind and Searl, 1978) which use the atmospheric line parameter data base of McClatchey et al. (1972). The spectral intervals used in Equation 1 range from 2 cm^{-1} through 2750 cm^{-1}. There is otherwise no need to make radiometric measurements at all frequencies in order to perform the calculation shown in Equation 1, except for the characterization of the frequency dependent terms $\alpha\varepsilon_{kj}$ and ε_j. In the TOVS Pathfinder data set, ε_j is taken as unity at all frequencies and $\alpha\varepsilon_{kj}$ is determined at 800 cm^{-1} for

each of two cloud layers k and is assumed to be independent of frequency in the calculation of OLR. No other approximations are made in the calculation of Equation 1.

OLR is computed using AIRS/AMSU sounding products in a completely analogous manner to that used for the TOVS Pathfinder Path-A data set, including use of the same Mehta and Susskind OLR RTA (Susskind et al. 2003). Products retrieved from AIRS are analogous to, and include, those contained in the TOVS Pathfinder Path A data set. AIRS measures IR channel radiances over the interval 650 cm^{-1} to 2668 cm^{-1}. The AIRS results shown below were derived using the AIRS Science Team Version-5 retrieval algorithm (Susskind et al., 2011a), in which the surface spectral emissivity ε_v is determined as a function of frequency, and band dependent surface emissivities ε_j are used in the OLR calculation. Surface emissivities at frequencies lower than 650 cm^{-1} are set equal to those at 650 cm^{-1} and are irrelevant with regard to the computation of OLR because the atmosphere is opaque at those frequencies. OLR_{CLR}, the clear sky OLR, is also a computed product obtained using Equation 1 but setting both $\alpha\varepsilon_1$ and $\alpha\varepsilon_2$ equal to zero. There is no need to observe clear spots to determine OLR_{CLR}.

2. AIRS and CERES OLR data sets used

In this paper we use the operational monthly mean OLR data products derived using the AIRS and CERES Science Team methodologies respectively. We obtained the AIRS OLR from the Goddard DISC and the CERES products from the Langley ASDC. AIRS was launched on the EOS Aqua satellite in a 1:30 AM/PM local crossing time orbit in May 2002. The operational processing of AIRS data began after AIRS became stable in September 2002. We use the AIRS Version-5 monthly mean Level-3

products, which is presented on a 1° x 1° latitude-longitude grid, and contains separate monthly mean products generated for each of the 1:30 AM local time, and 1:30 PM local time orbits. In this paper, we averaged the AM and PM products together to generate and use a single monthly mean product on the 1° x 1° grid for each month included in the data set.

CERES has flown on both EOS Terra, which was launched in December 1999 on a 10:30 AM/PM local crossing time orbit, as well as EOS Aqua, the same platform that carries AIRS. The CERES Science Team generates a number of different OLR data sets using CERES observations. The latest versions of the longest record CERES OLR data sets are referred to as the CERES SSF1deg-lite Ed2.5 data sets, which like AIRS, are presented on 1° x 1° latitude-longitude grid. At the time of this writing, the CERES Edition-2.5 OLR data sets extend to February 2010, and the AIRS Level-3 products extend to December 2010. CERES SSF1deg-lite Ed2.5 uses the latest calibration improvements (Priestley et al., 2011) with Edition2 CERES cloud retrievals (Minnis et al., 2008, Minnis et al., 2011), angular dependence models (Loeb et al., 2005), and time-space averaging (Young et al., 1998).

One would think it is more appropriate to compare AIRS OLR products with those obtained using CERES Aqua because AIRS and CERES Aqua are on the same satellite and measured at the same time of day, rather than comparing AIRS OLR with CERES Terra because AIRS and CERES Terra make measurements at different times of day. Nevertheless, the interannual variations of OLR during the 7½ years under study as reflected in both Terra and Aqua CERES data sets are much larger than any differences

due to the different observation times. As a result, spatial patterns of AIRS OLR anomalies can be compared with those of either CERES Terra or CERES Aqua.

Figure 1 shows global monthly mean values for AIRS OLR and also for CERES Aqua and CERES Terra Edition-2.5 OLR, henceforth referred to as CERES Aqua and CERES Terra OLR, for the overlap period September 2002 through February 2010. The AIRS OLR time series contains the symbol * on the months November 2003 and January 2010. Satellite data for these months were partially missing from the AIRS data record, and were generated synthetically, on a grid box by grid box basis, by setting grid point anomalies for a missing month to be equal to the average value of the corresponding anomalies of the previous and subsequent month. We use these synthetic OLR records as if they were actual observations in the subsequent discussion.

A number of features are apparent from Figure 1. The most prominent result is that the AIRS and CERES OLR data sets appear, to first order, to be biased compared to each other. Figure 2 shows the differences between the monthly global mean values of AIRS OLR and those of CERES Terra OLR and CERES Aqua OLR shown in Figure 1, as well as the difference between CERES Terra and CERES Aqua Global mean OLR. Each OLR difference time series also contains a dashed line showing the average value of the OLR difference. AIRS Version-5 OLR shows a nearly constant bias, with an average value of 9.06 W/m^2, compared to CERES Terra. There is a small essentially repetitive seasonal cycle, with maxima and minima in June and December respectively, in the difference between AIRS and CERES Terra OLR. The difference between AIRS and CERES Aqua OLR is similar to that between AIRS and CERES Terra OLR, but is somewhat more variable over time. CERES Terra OLR is slightly larger than CERES

Aqua OLR, especially before January 2005. As with AIRS OLR, there is a small mostly repetitive annual cycle in the difference between CERES Terra OLR and CERES Aqua OLR from 2005 on.

The nearly constant bias between OLR as computed based on AIRS products and observed by CERES is primarily a result of the use of an old set of line by line absorption coefficients in the parameterization of the Version-5 OLR RTA (Mehta and Susskind, 1999a,b). AIRS Version-6 uses an improved OLR RTA (Iacono et al., 2008) to compute OLR. This new RTA has two important improvements compared to Mehta and Susskind (1999a,b). Most significantly, the new OLR RTA is generated using more up to date line absorption parameters, especially for the very strong water vapor absorption band near 300 cm^{-1}. In addition, the new OLR calculation allows for inclusion of the effects of variations in CO_2 concentration over time, as well as those of other minor absorption species such as CO, CH_4, and N_2O, in the calculation of OLR. Appendix A gives additional details about improvements in the AIRS Science Team Version-6 retrieval system compared to Version-5, and shows that global mean values of AIRS Version-6 OLR should agree with CERES OLR to within 1 W/m^2.

Table 1 shows values of the slopes of the least squares linear fits to the differences AIRS minus CERES Terra OLR, AIRS minus CERES Aqua OLR, and CERES Terra minus CERES Aqua OLR, as well as the mean differences and standard deviations of these OLR time series over the period September 2002 through August 2009. The comparison statistics are given for this portion of the total overlap time period because it represents differences over a complete 7-year period. It is important that these slopes be compared over complete years to minimize artifacts due to effects of

the annual cycle differences in each data set. The slope of the differences between AIRS and CERES OLR records over this 7-year time period is not affected by a constant bias and gives a preliminary indication as to how well the Average Rate of Change (ARC) of anomalies of the different data sets will agree with each other, where the ARC for a given data set is defined as the slope of the linear least squares fit passing through an anomaly time series. We use the term Average Rate of Change to describe the slopes of anomaly time series rather than the term Trend, which has also been used to describe the slope of an anomaly time series, but is generally used to characterize long-term multi-decadal data sets rather than the 7 ½-year period studied in this paper. The slope for the time series AIRS minus CERES Terra OLR is considerably smaller than that of AIRS minus CERES Aqua OLR. The standard deviation between the AIRS OLR and CERES Terra OLR time series is also considerably smaller than that between AIRS OLR and CERES Aqua OLR, and closer to that between CERES Terra OLR and CERES Aqua OLR. This does not necessarily imply that the CERES Terra OLR record is in any way better than the CERES Aqua OLR record. For the purposes of this paper, we felt it was sufficient to show comparisons of anomaly time-series of AIRS OLR products with those of a single CERES OLR data set. Based on the results shown in Table 1, we chose to use the CERES Terra OLR product in OLR comparisons between CERES and AIRS shown in the remainder of this paper.

3. Comparison of AIRS and CERES Terra OLR Anomaly Time Series

This section compares the anomaly time series of CERES and AIRS OLR products over the 7 year 6 month overlap period, September 2002 through February

2010. We use data from the 7 year period September 2002 through August 2009 to generate monthly mean OLR climatologies, on a 1° x 1° spatial resolution, for each data set. The monthly mean climatologies, on a 1° x 1° spatial grid, for each month January through August are defined as the 7 year average of the data for that month for the years 2003 to 2009, and those for September through December use the average of those monthly observations for the years 2002 to 2008. The OLR anomaly for a given month in a given year, on a 1° x 1° spatial grid, is defined as the difference between its monthly mean OLR value and the monthly climatology for that grid box. The area mean anomaly for a given month is the cosine latitude weighted average of the grid box anomalies contained in the area under consideration (Global, Tropical, North America etc.). As stated previously, the Average Rate of Change (ARC) over a given area is defined as the slope of the linear least squares fit passing through the anomaly time series for that area. It is very important to note that each OLR data set under consideration, AIRS and CERES Terra, has its own monthly mean climatology. Therefore, the biases and small seasonal cycle differences between AIRS and CERES Terra OLR shown in Figure 2 will be removed from the different anomaly time series to the extent that they are constant in time.

Figure 3 shows the Global anomaly time series of AIRS OLR and CERES Terra OLR for the period under study, as well as the difference between the two sets of monthly mean anomalies. Figure 4 shows analogous results for Tropical mean (20°N to 20°S) anomalies. Table 2 shows the Global and Tropical mean values of ARC for AIRS OLR and CERES Terra OLR over this time period, the standard deviation between the two sets of Global and Tropical anomaly time series, and the temporal correlations

between each Global and each Tropical anomaly time series. The agreement of Global as well as Tropical anomalies and Average Rates of Change between the AIRS and CERES OLR records is very good. AIRS and CERES Average Rates of Change agree with each other to within about 0.02 $W/m^2/yr$. The standard deviation of the difference between the Global OLR anomaly time series is considerably smaller than that of the two OLR time series because the effects of the small essentially constant annual cycle in the differences between AIRS and CERES Terra OLR has been removed to first order in the generation of the anomaly time series. The temporal correlation of the two Global and Tropical OLR anomaly time series are 0.953 and 0.982 respectively. Both show that Global mean OLR has been decreasing, on the order of -0.1 $W/m^2/yr$, over the common time period September 2000 through February 2010, and Tropical mean OLR has been decreasing at a rate almost twice that amount.

Figure 3 shows that an onset of negative Global OLR anomalies begins in late 2007. Tropical OLR anomalies, shown in Figure 4, are in general considerably larger than Global anomalies, especially after mid-2007. It is apparent that the decrease in Global OLR in late 2007 arises primarily from the significant reduction in Tropical OLR which started a few months earlier. Tropical OLR anomalies, and to a lesser extent Global OLR anomalies, became positive starting in late 2009.

The Global and Tropical OLR anomaly time series are indeed very highly correlated with each other. The temporal correlation of the CERES Global and Tropical OLR anomaly time series with each other is 0.55, and the corresponding correlation for the AIRS time series is 0.57. This shows that what is happening in the tropics is a significant driver with regard to Global OLR anomalies. Susskind et al. (2011b) show

that both Tropical and Global OLR anomalies are strongly influenced by El Niño/La Niña cycles with El Niño time periods corresponding to positive Tropical and Global OLR anomalies, and La Niña time periods corresponding to negative OLR anomalies.

The Average Rates of Change (ARC's) shown in Table 2 are the slopes of the best linear fits to the anomaly time series shown in Figures 3 and 4. These anomaly time series do not vary linearly. Therefore values of the ARC's shown in Table 2 are dependent on the extent of the time series used in the generation of the linear least squares fit. Because both Global and Tropical anomalies are positive at the end of 2009, the negative OLR ARC's shown in Table 2 are less negative than they would have been if the time series used to compute ARC's were terminated earlier in the mission. Figure 5 shows a plot of values of AIRS and CERES Global and Tropical OLR ARC's, and their differences, computed over periods starting September 2002 and ending each month starting August 2006 and extending through February 2010. Both sets of Global and Tropical OLR ARC's computed as a function of ending time are always negative because of the positive anomalies at the start of the time period, which occurred during an El Niño (Susskind et al., 2011b). The maximum time dependent negative Average Rate of Change occurred in March 2009 for both Global and Tropical OLR. The time series of Global AIRS and Global CERES ARC's computed as a function of ending time period have a correlation of 0.966, and those of the Tropical ARC's have a correlation of 0.982. The time series of AIRS Global ARC's and AIRS Tropical ARC's computed as a function of ending time are also highly correlated with each other, with a correlation coefficient of 0.77. This is a further indication that tropical anomalies play a

large role with regard to Global ARC's. All ARC's shown in the rest of this paper refer to ARC's derived for the period September 2002 through February 2010.

Figure 6 shows the zonal mean ARC's of the AIRS and CERES Terra OLR records for the period September 2002 through February 2010, as well as the difference of the two sets of ARC's. There is again excellent agreement between the zonal mean structure of ARC's in both OLR data sets, which have a latitudinal correlation of 0.96. It is apparent from Figure 6 that the majority of the decrease in Global OLR during the time period under study originates in the tropics south of 5°N. Other areas of negative OLR ARC's occur near 60°S and 60°N latitudes. OLR increased over this time period north of 70°N. AIRS negative zonal mean OLR ARC's are somewhat larger than those of CERES between the 5°S and 45°S and AIRS OLR ARC's are more positive (or less negative) than those of CERES poleward of 70°.

The spatial distributions of Global OLR ARC's over the time period September 2002 through February 2010 are shown in Figures 7a and 7b for AIRS and CERES Terra respectively. Both fields are presented on the 1° latitude by 1° longitude grid on which the data sets are given. Figures 7a and 7b demonstrate two very important points. The first is that the spatial distributions of the ARC's of AIRS OLR and of CERES Terra OLR are virtually indistinguishable from each other. Figure 7c shows the spatial distribution of the difference between the two sets of ARC's. The spatial correlation between the two sets of ARC's is 0.971 and the spatial standard deviation of the two sets of ARC's is 0.15 $W/m^2/yr$. The global AIRS OLR ARC for the period September 2002 through February 2010 is 0.027 $W/m^2/yr$ lower (more negative) than that of CERES Terra. This small difference is not monolithic, but occurs primarily near 30°S

latitude, especially over Eastern Australia and South Africa, both of which contain large negative OLR ARC's. In other words, the large negative OLR ARC's in these regions are slightly larger in AIRS than in CERES, which may or may not be an artifact in the AIRS data. The same amplification of local OLR ARC's (positive and negative) in AIRS compared to CERES is found in a number of other locations as well.

The second major point of Figures 7a and 7b is that while OLR Average Rates of Change do show a pronounced zonal mean structure, there is considerable longitudinal structure at given latitudes as well. This longitudinal structure is particularly noteworthy in the tropics. As shown in Figure 6, zonal mean Tropical OLR ARC's are very negative, but positive OLR ARC's, as large as 3.1 $W/m^2/yr$ exist in the vicinity of the equatorial dateline. These are more than compensated for, in the zonal mean sense, by negative OLR ARC's at other longitudes, as large as -2.8 $W/m^2/yr$ near the equator.

Figures 8a and 8b show Hovmöller diagrams presenting time series of monthly mean OLR anomalies (vertical scale), integrated over the latitude range 5°N through 5°S, in each 1° longitude bin (horizontal scale) for the period September 2002 through February 2010. The difference between these two figures is shown in Figure 8c. These figures have a small amount of smoothing applied to them. A five point (5 month) smoothing was applied in the vertical and a fifteen point (15 degree) smoothing was applied in the horizontal to minimize the effects of small discontinuities between adjacent rectangular grid points on the figures. Most of the region covered is ocean. There are three relatively small land areas near the equator: South America, Africa, and Indonesia. These land areas each lie between the three sets of narrow vertical lines shown in Figure 8. The two sets of Hovmöller diagrams are essentially identical, with a

correlation coefficient of 0.993 between them. Some of the largest differences between the AIRS and CERES tropical anomaly time-series occur in November 2003 and January 2010, the two months for which AIRS data was synthesized. These differences would have been much larger if the AIRS “monthly mean” OLR products stored at the Goddard DISC were used in the calculations, because in both cases the AIRS “monthly mean” products represented averages over less than a month time period while the CERES data represented observations taken over the entire month. Indeed, when the AIRS data contained at the DISC for these two months was used originally in the generation of Figure 8, those two months showed pronounced signals in the original Figure 8C. This alerted us to check, and correct for, the cause of this problem.

4. Summary

This paper compares spatial and temporal OLR anomalies over the time period September 2002 through February 2010 and their Average Rates of Change as observed by CERES and computed based on AIRS retrieved surface and atmospheric geophysical parameters. Taken together, Figures 3 to 8 show that the spatial patterns of the AIRS and CERES Average Rates of Change over that time period are essentially in perfect agreement with each other, as are the anomaly time series averaged over different spatial regions. Both CERES and AIRS OLR products show that the time period under study is marked by a substantial decrease in global OLR, on the order of $-0.10\ \mathrm{W/m^2/yr}$, averaged over the globe, as well as a decrease on the order of $-0.17\ \mathrm{W/m^2/yr}$ averaged over the tropics. There are very large spatial variations of these Average Rates of Change however, with local values ranging from $-2.8\ \mathrm{W/m^2/yr}$ to $+3.1\ \mathrm{W/m^2/yr}$ in the tropics. Global and Tropical OLR both began to decrease

significantly at the onset of a strong La Niña in late 2007. This essentially perfect agreement of OLR anomaly time series derived from observations by two different instruments, in totally independent and different manners, implies that both sets of results must be highly accurate. There is no question that there actually was a decrease of Global mean OLR on the order of 0.1 W/m^2/yr over the time period September 2002 through February 2010, and that the majority of the decrease occurred in the tropics. This result should not be taken as indicative in any way as to what will happen in the future. It only shows that OLR anomalies and their Average Rate of Change can be determined very accurately by two totally independent instrumental and theoretical approaches. The agreement of anomaly time series of OLR as observed by CERES and computed from AIRS derived products also indirectly validates the anomaly time series of the AIRS derived products used in the computation of AIRS OLR. Moreover, it further indicates that anomaly time series of AIRS derived products can be used to explain the factors contributing to anomaly time series of OLR. Susskind et al. (2011b) use anomaly time series of AIRS Version-5 surface skin temperature, water vapor profiles, and cloud cover to show that the large negative decrease in Global OLR over the time period under study is primarily a result of the phases of El Niño/La Niña oscillations and their effects on the distribution of water vapor and cloud cover in the tropics, particularly in the region bounded by 8°N latitude and 20°S, and 140°W eastward to 40°E longitude.

The combination of results shown in this paper and in Susskind et al. (2011b) shows the importance of maintaining AIRS and CERES capabilities, or better, well into the future. If there were only a CERES (or AIRS) OLR product, one could be skeptical

regarding OLR Average Rates of Change derived from one or the other data set as they could be a result of instrumental or computational artifacts. It is extremely unlikely that OLR Average Rates of Change obtained in two totally different manners, using two independent instrumental approaches, would agree to within ± 0.01 $W/m^2/yr$ if each approach had their own significant artifacts.

While the agreement of anomaly time series of OLR computed using AIRS Version-5 products and observed in CERES Edition-2.5 processing is extremely significant, it is still somewhat disconcerting that there is a bias on the order of 9.1 W/m^2 between the two sets of OLR products. The source of this bias has been identified and will be corrected in the AIRS Science Team Version-6 retrieval algorithm, expected to become operational in mid to late 2011. The AIRS Version-6 retrieval system will have a number of improvements compared to AIRS Version-5. We briefly describe the improvements most relevant to the calculation of OLR in Appendix A. Appendix A shows that AIRS Version-6 OLR should agree with CERES Edition-2.5 OLR to within 1 W/m^2, corroborating not only CERES OLR anomalies and their Average Rates of Change, but the absolute value of CERES OLR as well.

Appendix A: Improved OLR Calculation in AIRS Version-6

The AIRS Science Team Version-6 retrieval algorithm should become operational at the Goddard DISC in mid to late 2011. AIRS Version-6 will have a number of improvements compared to Version-5. From the OLR perspective, the most important change is the use of an improved OLR RTA (Iacono et al., 2008) to compute OLR . This new RTA has two important improvements compared Mehta and Susskind (1999a,b). Most significantly, the new RTA is generated using more up to date line absorption parameters, especially for the very strong water vapor absorption band near 300 cm^{-1}. In addition, the new OLR calculation allows for inclusion of the effects of variations in CO_2 concentration over time, as well as those of other minor absorption species such as CO, CH_4, and N_2O, in the calculation of OLR. The Version-5 OLR RTA did not include these effects and parameterized atmospheric transmittances only in terms of variable temperature, water vapor, and ozone. Consequently, the Version-5 OLR calculation could not allow for the effects of the increase in CO_2 over the time period under study on computed values of OLR. Version-6 does not solve for variable CO_2, but it uses a climatological value of CO_2 mixing ratio, which increases linearly at a rate of 2.03 ppm per year, in its OLR calculation.

Version-6 OLR will also contain an important set of new OLR related products. As shown in Equation 1, Version-5 OLR is computed as a sum of fluxes in 14 contiguous spectral intervals. Version-6 OLR uses a similar methodology to compute OLR as a sum of fluxes over 16 contiguous spectral intervals. AIRS Science Team products are derived consistent with AMSU observations in a given AMSU-A footprint and the ensemble of AIRS observations in each of the 3x3 array of AIRS Fields of View

(FOV's) contained within the AMSU-A footprint, referred to as the AIRS Field of Regard (FOR). Most AIRS Science Team products are generated on an AIRS FOR basis, but individual cloud products are generated for each AIRS FOV. Version-6 will compute and write out level-2 spot-by-spot OLR products for each AIRS FOV, while Version-5 computed and wrote out OLR only for the AIRS FOR. Version-6 will also compute and store level-2 spot-by-spot products and level-3 gridded products, not only for OLR, as done currently, but also for each of its 16 spectral components. This will allow for the study of anomalies and Average Rates of Change of the fluxes in each of the subbands, as well as for the total longwave flux as done currently.

The AIRS Science Team Version-6 algorithm also has a number of other improvements in retrieval methodology which will affect the OLR product. The major improvement in Version-6 products compared to Version-5 is a result of new methodology to determine surface skin temperature and surface spectral emissivity, especially during the day (Susskind et al., 2009). In addition, Version-6 cloud products and OLR are derived separately for each of the nine AIRS FOV's within an AMSU footprint, as opposed to being derived once per AMSU footprint in Version-5. Version-6 retrieved cloud parameters are also improved compared to Version-5, especially for very cloudy cases.

The latest version of the AIRS Version-6 retrieval algorithm has been tested on six days in different years and different seasons, ranging from September 6, 2002 thorugh August 10, 2007. Figure A1a shows the 1:30 AM/PM average of Version-6 OLR for September 6, 2002 and Figure A1b shows Version-6 OLR minus Version-5 OLR for this day. Cloudy regions are generally characterized by having lower OLR than

surrounding areas. Version-6 Global mean OLR for this day is 9.61 W/m^2 lower than Version-5 OLR. The difference in OLR between the two versions has significant spatial variability. In some cloudy areas, such as the region surrounding 60°S, 100°W, Version-6 OLR is actually somewhat higher than Version-5 OLR, while in the equatorial area east of the dateline, Version-6 OLR is considerably lower than Version-5 OLR.

Figure A2a shows the spatial distribution of the 6-day average of OLR computed using Version-6 and Figure A2b shows its difference from the 6-day average Version-5 OLR product. The most important point to notice is that the Version-6 global mean OLR averaged over six days is lower by 9.20 W/m^2 than the Version-5 global mean OLR product. This indicates that AIRS Version-6 global mean OLR should agree with CERES Edition-2.5 OLR to within about 1 W/m^2. The largest decreases in Version-6 OLR compared to Version 5 occur in the tropics, which contains the most water vapor. This is a result of the improved flux calculation in the rotational water vapor band. Differences in regions containing high clouds on one or more of the six days are smaller, even in the tropics, because there is less atmospheric water vapor above the clouds. Other local differences between Version-6 and Version-5 OLR are primarily the result of changes in retrieved cloud and surface skin parameters.

References:

Allan, R. P., and M. A. Ringer, 2003: Inconsistencies between satellite estimates of longwave cloud forcing and dynamical fields from reanalyzes. *Geophys. Res. Lett.*, **30,** 4.

Barkstrom, B., E. Hrrision, G. Smith, R. Green, J. Kibler, R. Cess, the ERBE Science Team,1989: Earth Radiation Budget (ERBE) Archival and April 1985 Results. *Bulletin of the American Meteorological Society*, **70**, 1254-1262.

Barlow, M., M. Wheeler, B. Lyon, and H. Cullen, 2005: Modulation of daily precipitation over southwest Asia by the Madden-Julian oscillation. *Mon. Weather Rev.*, **133,** 3579-3594.

Chiodi, A. M., and D. E. Harrison, 2010: Characterizing Warm-ENSO Variability in the Equatorial Pacific: An OLR Perspective. *J. Clim.*, **23,** 2428-2439.

Chu, P. S., and J. B. Wang, 1997: Recent climate change in the tropical western Pacific and Indian Ocean regions as detected by outgoing longwave radiation records. *J. Clim.*, **10,** 636-646.

Chung, E. S., D. Yeomans, and B. J. Soden, 2010: An assessment of climate feedback processes using satellite observations of clear-sky OLR. *Geophys. Res. Lett.*, **37,** 7.

Fasullo, J. T., and K. E. Trenberth, 2008: The annual cycle of the energy budget. Part II: Meridional structures and poleward transports. *J. Clim.*, **21,** 2313-2325.

Gruber, A., R. Ellingson, P. Ardanuy, M. Weiss, S. K. Yang, and S. N. Oh, 1994: A COMPARISON OF ERBE AND AVHRR LONGWAVE FLUX ESTIMATES. *Bulletin of the American Meteorological Society*, **75,** 2115-2130.

Hoyos, C. D., and P. J. Webster, 2007: The role of intraseasonal variability in the

nature of Asian monsoon precipitation. *J. Clim.*, **20,** 4402-4424.

Huang, Y., and V. Ramaswamy, 2009: Evolution and Trend of the Outgoing Longwave Radiation Spectrum. *J. Clim.*, **22,** 4637-4651.

Iacono, M. J., J. S. Delamere. E. J. Mlawer, M. W. Shephard, S. A. Clough, and W. D. Collins, 2008: Radiative Forcing by Long-Lived Greenhouse Gases: Calculations with the AER Radiative Transfer Models. *Jour. of Geophy. Res*., **113**, D13103, doi:10.1029/2008JD009944.

Jacobowitz, H., H. V. Soule, H. L. Kyle, F. B. House, and the ERBE Nimbus 7 Experiment Team, 1984: The Earth Radiation Budget (ERB) experiment: an overview. *J. Geophys. Res*., **89**, 5021-5038.

Jones, C., L. M. V. Carvalho, R. W. Higgins, D. E. Waliser, and J. K. E. Schemm, 2004: Climatology of tropical intraseasonal convective anomalies: 1979-2002. *J. Clim.*, **17,** 523-539.

Kidson, J. W., M. J. Revell, B. Bhaskaran, A. B. Mullan, and J. A. Renwick, 2002: Convection patterns in the tropical Pacific and their influence on the atmospheric circulation at higher latitudes. *J. Clim.*, **15,** 137-159.

Kiladis, G. N., K. H. Straub, and P. T. Haertel, 2005: Zonal and vertical structure of the Madden-Julian oscillation. *Journal of the Atmospheric Sciences*, **62,** 2790-2809.

Kyle, H. L., J. R. Hickey, P. E. Ardanuy, H. Jacobowitz, A. Arking, G. G. Campbell, F. B. House, R. Maschhoff, G. L. Smith, L. L. Stowe, and T. Vonder Haar, 1993: The Nimbus Earth Radiation Budget (ERB) Experiment: 1975-1992. *Bull. Am. Meteorol. Soc*., **74**, 815-830.

Loeb, N. G., S. Kato, K. Loukachine, and N. Manalo-Smith, 2005: Angular Distribution

Models for Top-of-atmosphere Radiative Flux Estimation from the Clouds and the Earth's Radiant Energy System Instrument on the Terra Satellite. Part 1: Methodology. *J. Atmos. Ocean. Tech*., **22**(4), 338-351.

McClatchey, R. A., R. W. Fenn, J. E. A. Selby, F. E. Volz, and J. S. Garing, 1972: Optical Properties of the Atmosphere (Third Edition). *Environ. Res. Papers*, **411**, AFCRL, Bedford, MA, 108 pp.

Mehta, A. V. and J. Susskind, 1999a: Outgoing Longwave Radiation from the TOVS Pathfinder Path A Data Set. *J. of Geophys. Res*., **104**, 12193-12212.

Mehta, A. V. and J. Susskind, 1999b: Longwave Radiative Flux Calculations in the TOVS Pathfinder Path A Data Set. *NASA Tech. Rep., GSFC/CR-1999-208643*.

Proc. SPIE International Symp. Infrared Spaceborne Remote Sensing and Instrumentation XVII, San Diego, CA, August 2009.

Minnis, P., Q. Z. Trepte, S. Sun-Mack, Y. Chen, D. R. Doelling, et al., 2008: Cloud Detection in Non-polar Regions for CERES Using TRMM VIRS and Terra and Aqua MODIS Data. *IEEE Trans. Geosci. Remote Sens*., **46**, 3857-3884.

Minnis, P., S. Sun-Mack, D. F. Young, P. W. Heck, D. P. Garber, et al., 2011: CERES Edition-2 Cloud Property Retrievals Using TRMM VIRS and Terra and Aqua MODIS data. Part 1: Algorithms. *IEEE Trans. Geosci. Remote Sens*. (in press).

Soden, B. J., and I. M. Held, 2006: An Assessment of Climate Feedbacks in Coupled Ocean–Atmosphere Models. *J. Clim.*, **19,** 3354-3360.

Susskind, J. and J. E. Searl, 1978: Synthetic Atmospheric Transmittance Spectra Near 15 μm and 4.3 μm. *J. Quant. Spectr. Rad. Trans*., **19**, 195-215.

Susskind, J., P. Piraino, L. Rokke, L. Iredell, and A. V. Mehta, 1997: Characteristics of

the TOVS Pathfinder Path A Data Set. *Bull. of Amer. Meteorol. Soc*., **78**, 1449-1472.

Susskind, J., C.D. Barnet, J.M. Blaisdell, 2003: Retrieval of atmospheric and surface parameters from AIRS/AMSU/HSB data in the presence of clouds. IEEE Transactions on Geoscience and Remote Sensing, Issue 2, **41**, Digital Object Identifier 10.1109/TGRS.2002.808236, 390-409.

Susskind, J., J. Blaisdell, and L. Iredell, 2009: Improved Determination of Surface and Atmospheric Temperatures Using Only Shortwave AIRS Channels. *Proc. SPIE International Symp. Infrared Spaceborne Remote Sensing and Instrumentation XVII*, San Diego, CA, August 2009.

Susskind, J., J. M. Blaisdell, L. Iredell, and F. Keita, 2011a: Improved Temperature Sounding and Quality Control Methodology Using AIRS/AMSU Data: The AIRS Science Team Version 5 Retrieval Algorithm. Geoscience and Remote Sensing, IEEE Transactions on Geoscience and Remote Sensing, Issue: 99 Digital Object Identifier: 10.1109/TGRS.2010.2070508, Publication Year: 2011, 1-25.

Susskind, J., G. Molnar, and L. Iredell, 2011b: The Effect of El Niño/La Niña Oscillations on Recent Anomaly Time Series of OLR. Submitted to *J. Climate*.

Wielicki, B. A., B. R. Barkstrom, E. F. Harrison, R. B. Lee III, G. L. Smith, and J. E. Cooper, 1996: Clouds and the Earth's Radiant Energy System (CERES): An Earth Observing System Experiment. *Bull. Amer. Meteor. Soc*., **77**, 853-868.

Young, D. F., P. Minnis, D. R. Doelling, G. G. Gibson, and T. Wong, 1998: Temporal Interpolation Methods for the Clouds and the Earth's Radiant Energy System (CERES) Experiment. *Jour. of Applied Meteor*., **37**(6), 572-590.

Table 1. Comparison of Global OLR Time Series
September 2002 through August 2009

	AIRS Minus CERES Terra	AIRS Minus CERES Aqua	CERES Terra Minus CERES Aqua
Slope [W/m^2/yr]	-0.0191	-0.0681	-0.0497
Mean [W/m^2]	9.07	9.53	0.46
Standard Dev.[W/m^2]	0.345	0.475	0.243

Statistical comparisons of anomaly time series for the period September 2002 through August 2009 for AIRS minus CERES Terra OLR, AIRS minus CERES Aqua OLR, and CERES Terra minus CERES Aqua OLR. Shown are the slopes of the least squares linear fits, and mean differences and standard deviations of the different OLR time series.

Table 2. OLR Anomaly Time Series Comparison
September 2002 through February 2010

Data Set	Global	Tropical
AIRS ARC (W/m^2/yr)	−0.1111 ± 0.0025	−0.1795 ± 0.0059
CERES Terra ARC (W/m^2/yr)	−0.0837 ± 0.0022	−0.1645 ± 0.0056
AIRS Minus CERES STD (W/m^2)	0.151	0.216
AIRS/CERES Correlation	0.953	0.982

Global and Tropical statistical comparisons of OLR anomaly time series for the period September 2002 through February 2010 for AIRS and CERES Terra OLR. Shown are the Average Rates of Change, the standard deviations between the anomaly time series, and the temporal correlations of the anomaly time series.

Figure and Table Captions

Figure 1

Global monthly mean OLR from Version-5 AIRS and Edition-2.5 CERES aboard Aqua and Terra for the overlap period September 2002 through February 2010.

Figure 2

Global monthly mean OLR differences among AIRS, CERES Terra, and CERES Aqua; and dashed line showing the average value of each OLR difference for the overlap period September 2002 through February 2010.

Figure 3

Global monthly mean OLR anomaly time series and anomaly differences of AIRS and CERES Terra for the overlap period September 2002 through February 2010.

Figure 4

Tropical (20°N to 20°S) monthly mean OLR anomaly time series and anomaly differences of AIRS and CERES Terra for the overlap period September 2002 through February 2010.

Figure 5

AIRS and CERES Global and Tropical OLR Average Rates of Change and their differences, computed over varying time intervals, each starting in September 2002 and ending with varying time periods from August 2006 and extending through February 2010.

Figure 6

Zonal mean Average Rates of Change (ARC's) for AIRS and CERES Terra OLR monthly mean time series for the period September 2002 through February 2010, as well as the difference of the two sets of ARC's. The majority of the decrease in Global OLR during this period originates in the tropics south of 5°N.

Figure 7

Spatial 1° latitude by 1° longitude distributions of Global OLR ARC's over the time period September 2002 through February 2010. Figures 7a shows the ARC for AIRS Version-5, 7b for CERES Terra Edition-2.5 , and 7c the difference of the two.

Figure 8

Hovmöller diagrams for time series of monthly mean OLR anomalies integrated over the latitude range 5°N through 5°S, in each 1° longitude bin for the period September 2002 through February 2010. Figure 8a shows the OLR anomalies for AIRS Version-5, 8b for CERES Terra Edition-2.5 , and 8c the difference of the two.

Figure A1a

The spatial distribution of 1:30 AM/PM average OLR computed for September 6, 2002 using the current version of the AIRS Science Team Version-6 retrieval algorithm.

Figure A1b

The AIRS Science Team Version-6 OLR minus Version-5 OLR for 1:30 AM/PM average of September 6, 2002.

Figure A2a

The AIRS Science Team Version-6 OLR for 1:30 AM/PM average of September 6, 2002, January 25, 2003, September 29, 2004, August 5, 2005, February 24, 2007, and August 10, 2007.

Figure A2b

The AIRS Science Team Version-6 OLR minus Version-5 OLR for the 1:30 AM/PM average of the six day period.

Table-1

Statistical comparisons of anomaly time series for the period September 2002 through August 2009 for AIRS minus CERES Terra OLR, AIRS minus CERES Aqua OLR, and CERES Terra minus CERES Aqua OLR. Shown are the slopes of the least squares linear fits, and mean differences and standard deviations of the different OLR time series.

Table-2

Global and Tropical statistical comparisons of OLR anomaly time series for the period September 2002 through February 2010 for AIRS and CERES Terra OLR. Shown are

the Average Rates of Change, the standard deviations between the anomaly time series, and the temporal correlations of the anomaly time series.

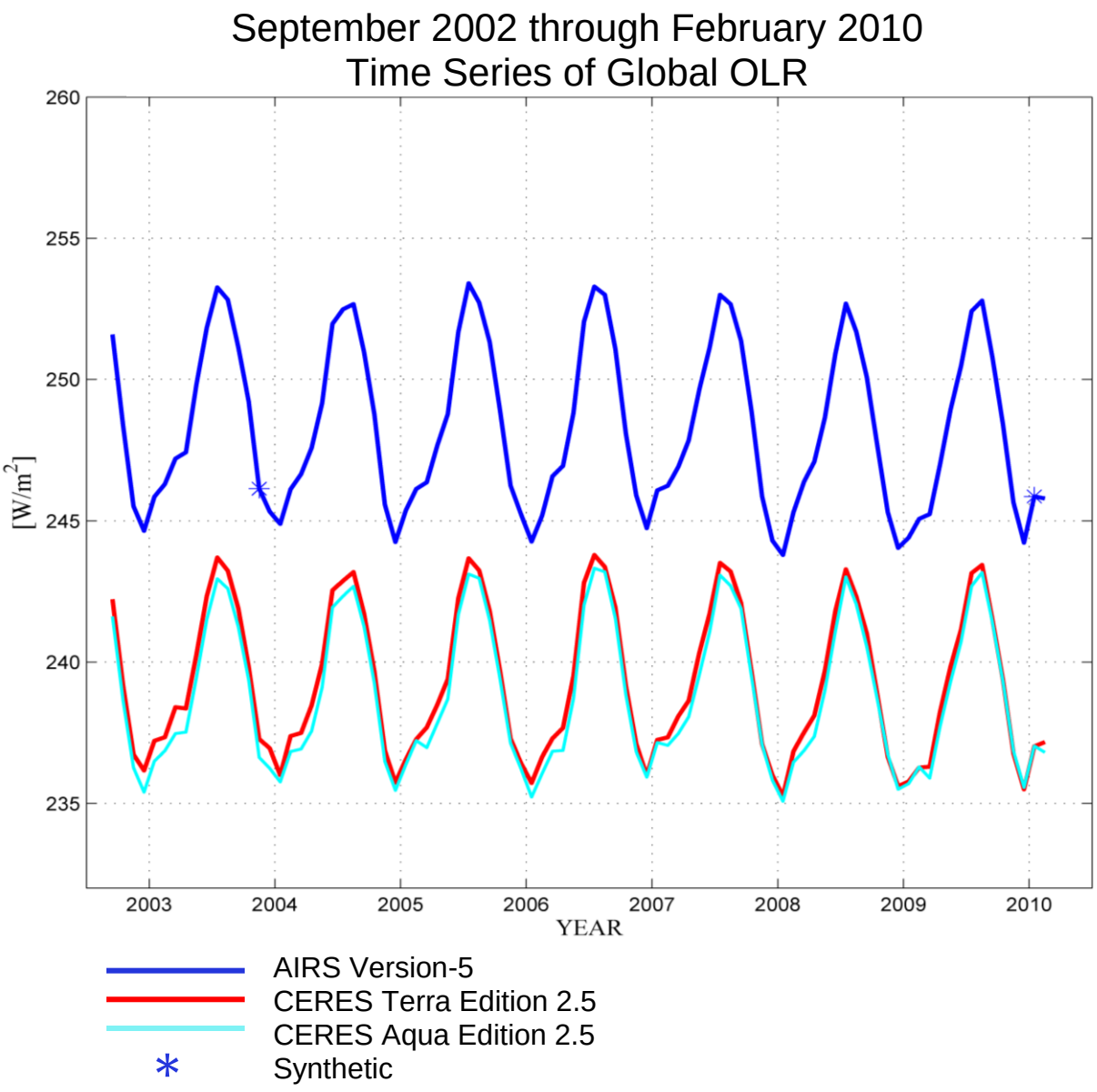

Figure 1. Global monthly mean OLR from Version-5 AIRS and Edition-2.5 CERES aboard Aqua and Terra for the overlap period September 2002 through February 2010.

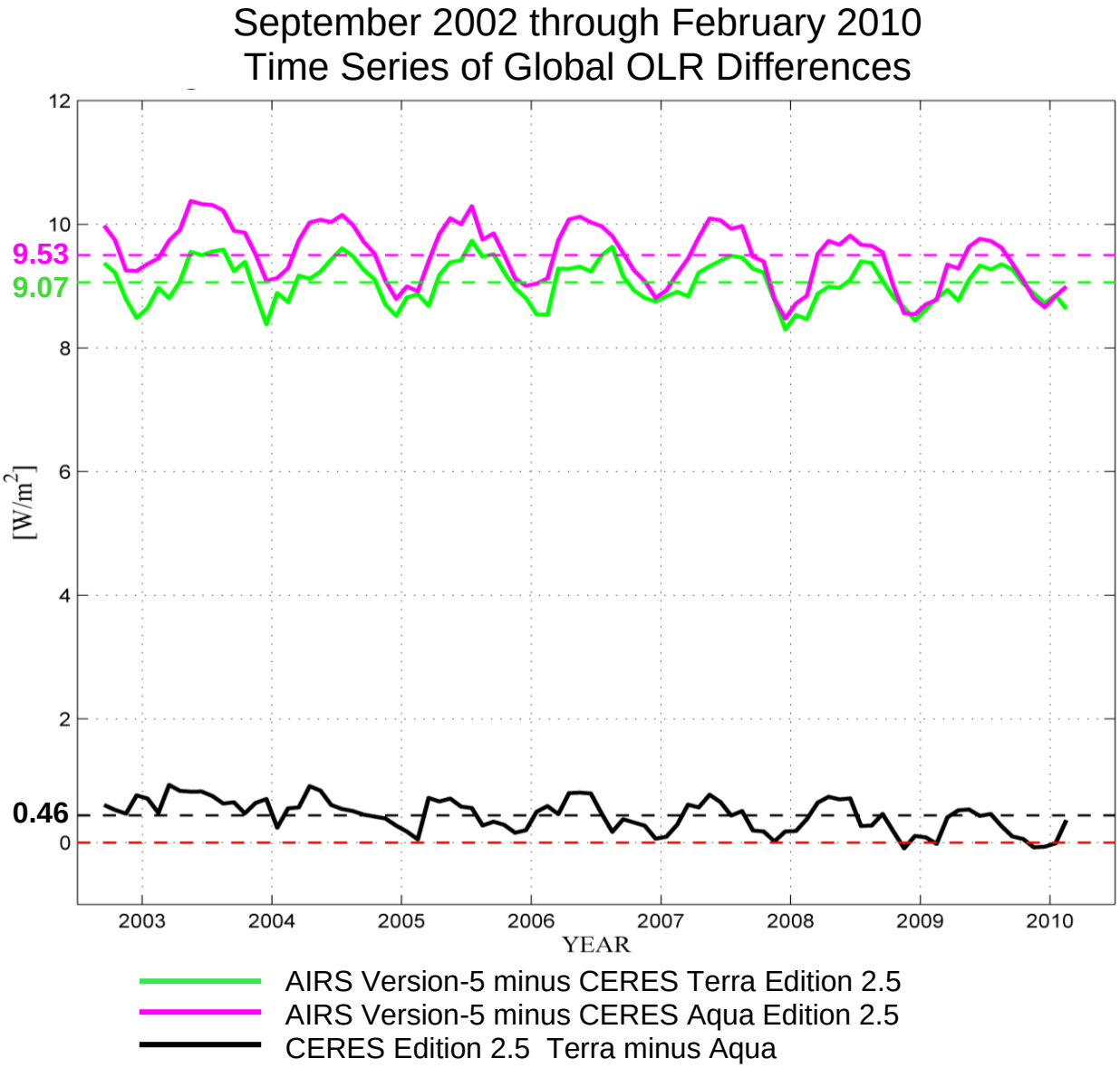

Figure 2. Global monthly mean OLR differences among AIRS, CERES Terra, and CERES Aqua; and dashed line showing the average value of each OLR difference for the overlap period September 2002 through February 2010.

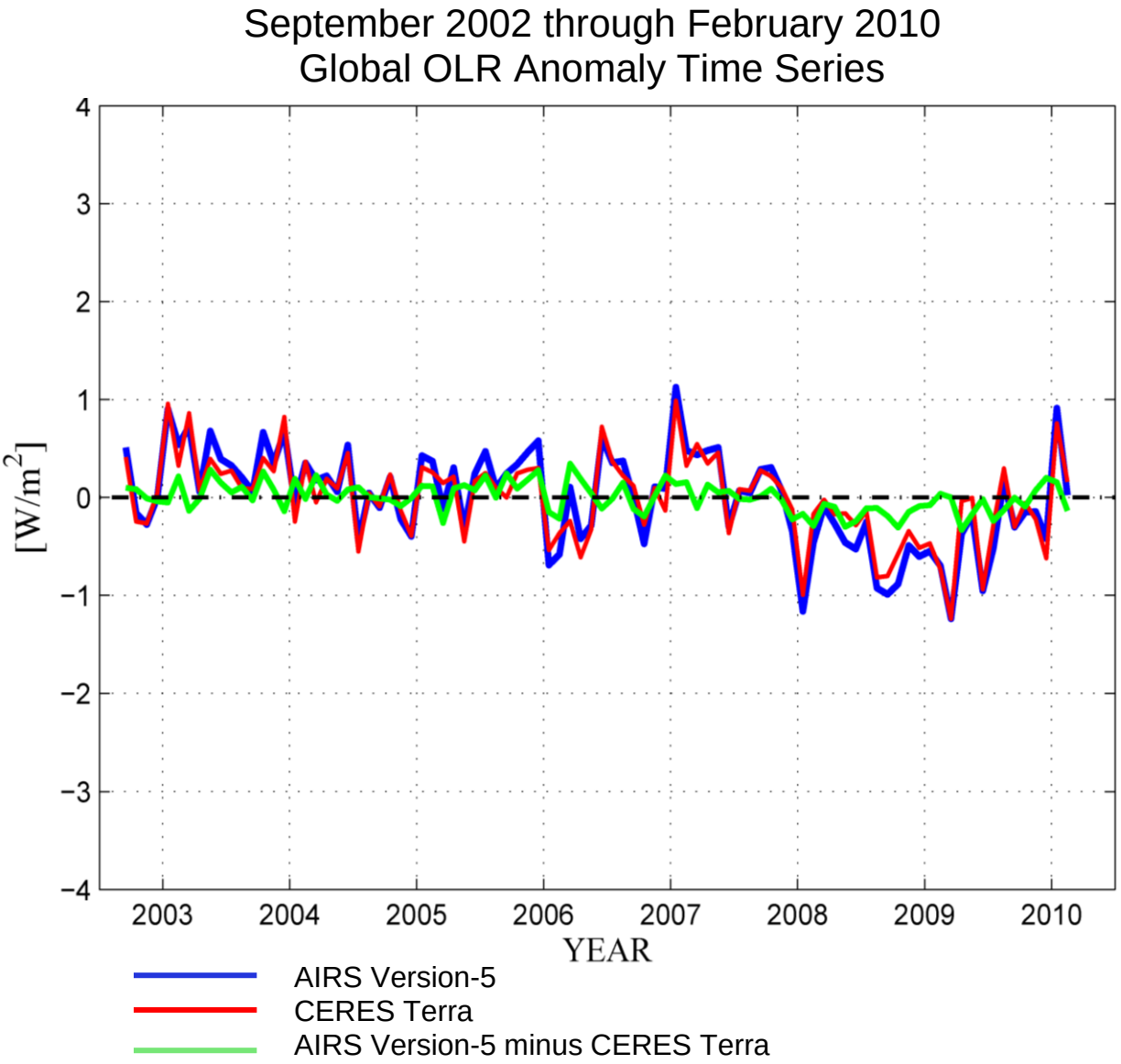

Figure 3. Global monthly mean OLR anomaly time series and anomaly differences of AIRS and CERES Terra for the overlap period September 2002 through February 2010.

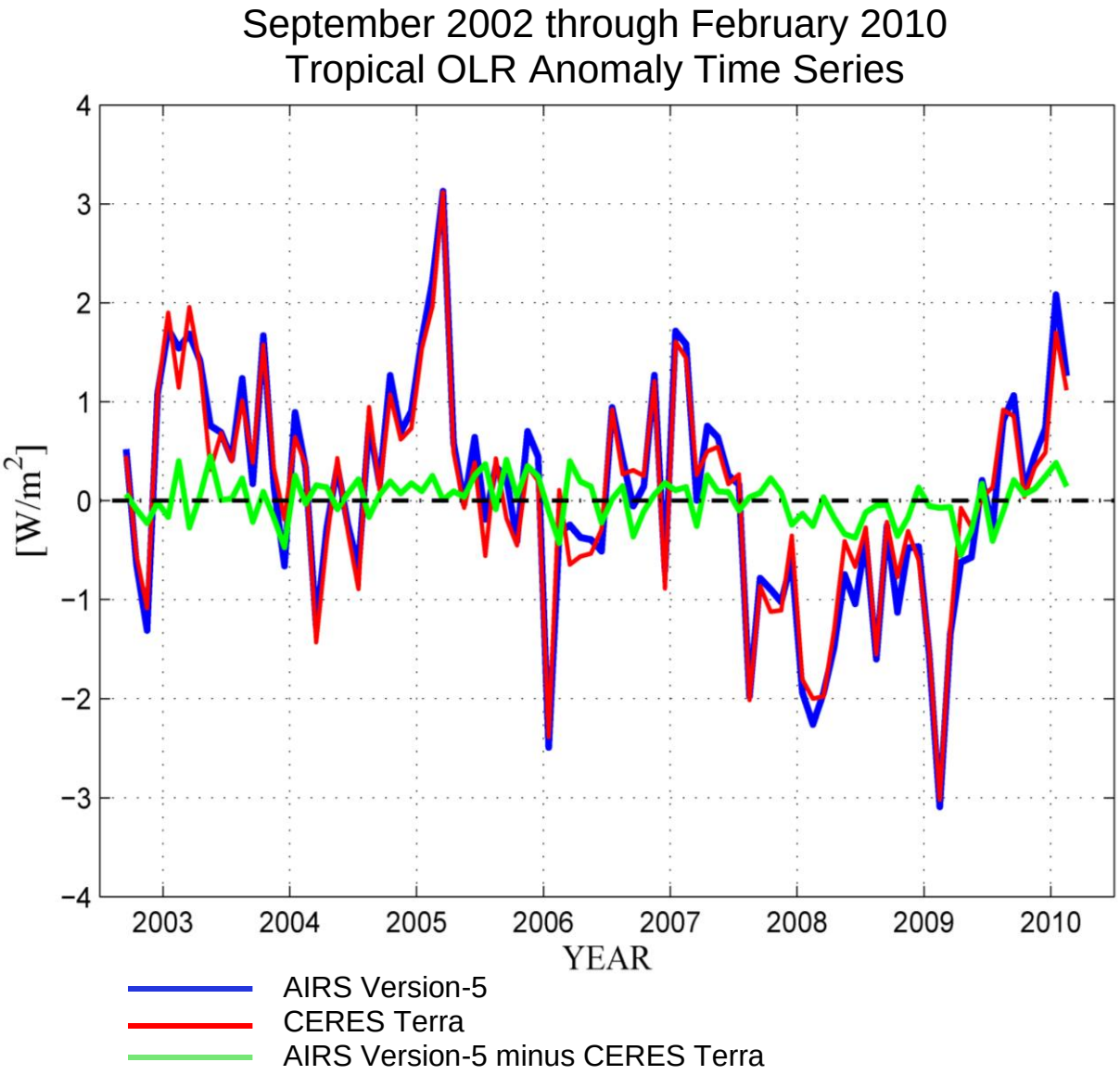

Figure 4. Tropical (20°N to 20°S) monthly mean OLR anomaly time series and anomaly differences of AIRS and CERES Terra for the overlap period September 2002 through February 2010.

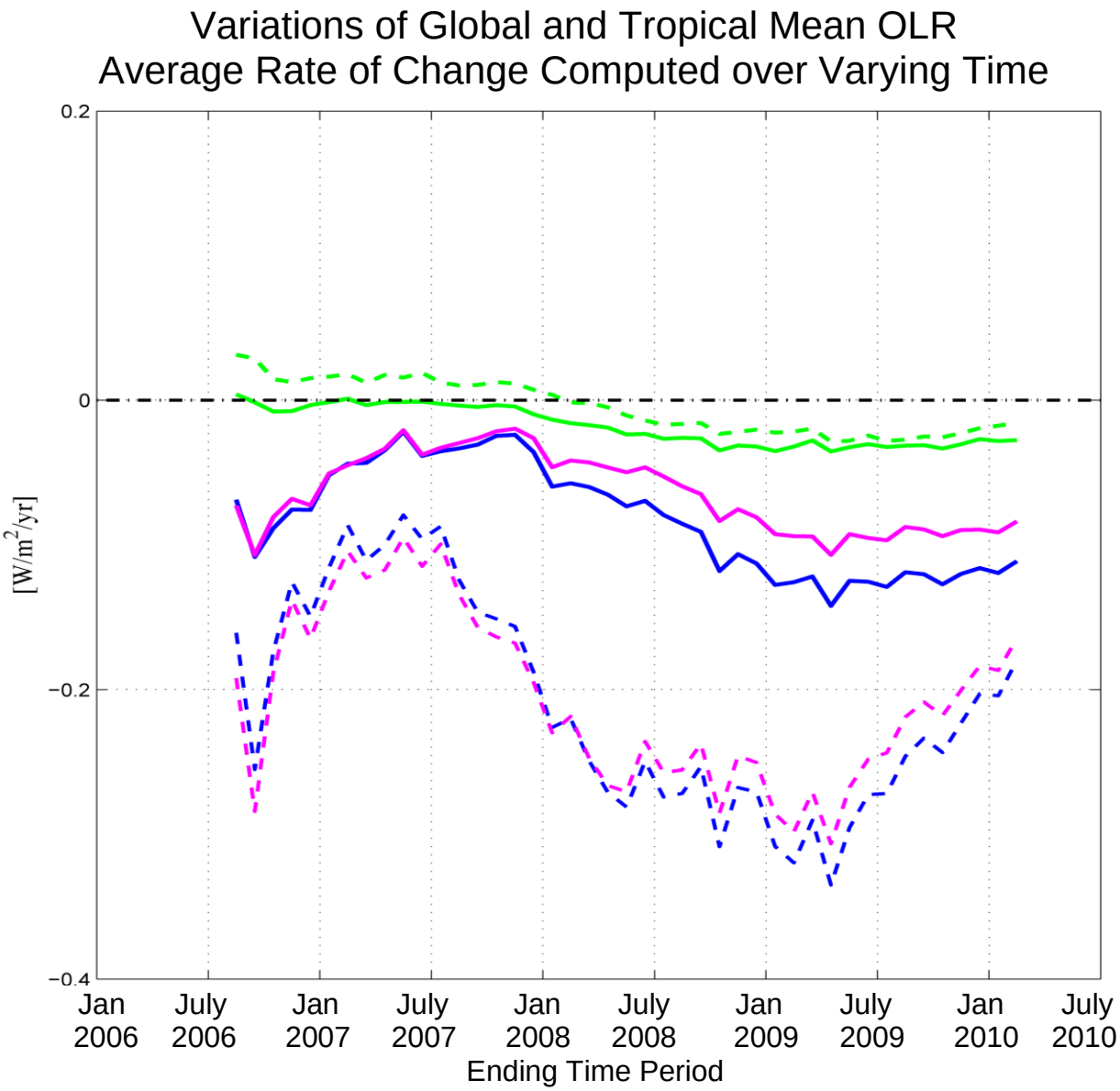

Figure 5. AIRS and CERES Global and Tropical OLR Average Rates of Change and their differences, computed over varying time intervals, each starting in September 2002 and ending with varying time periods from August 2006 and extending through February 2010.

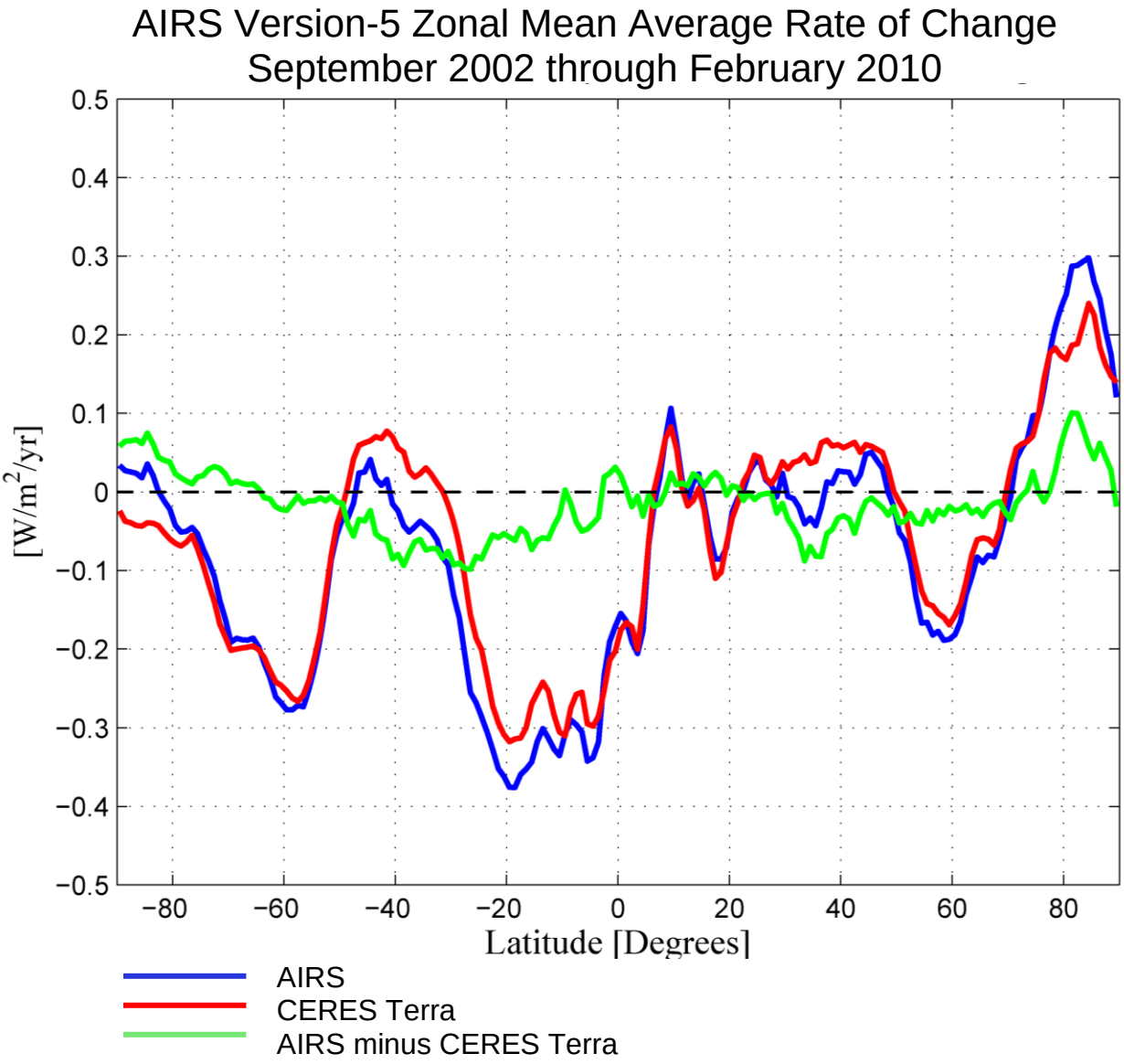

Figure 6. Zonal mean Average Rates of Change (ARC's) for AIRS and CERES Terra OLR monthly mean time series for the period September 2002 through February 2010, as well as the difference of the two sets of ARC's. The majority of the decrease in Global OLR during this period originates in the tropics south of 5°N.

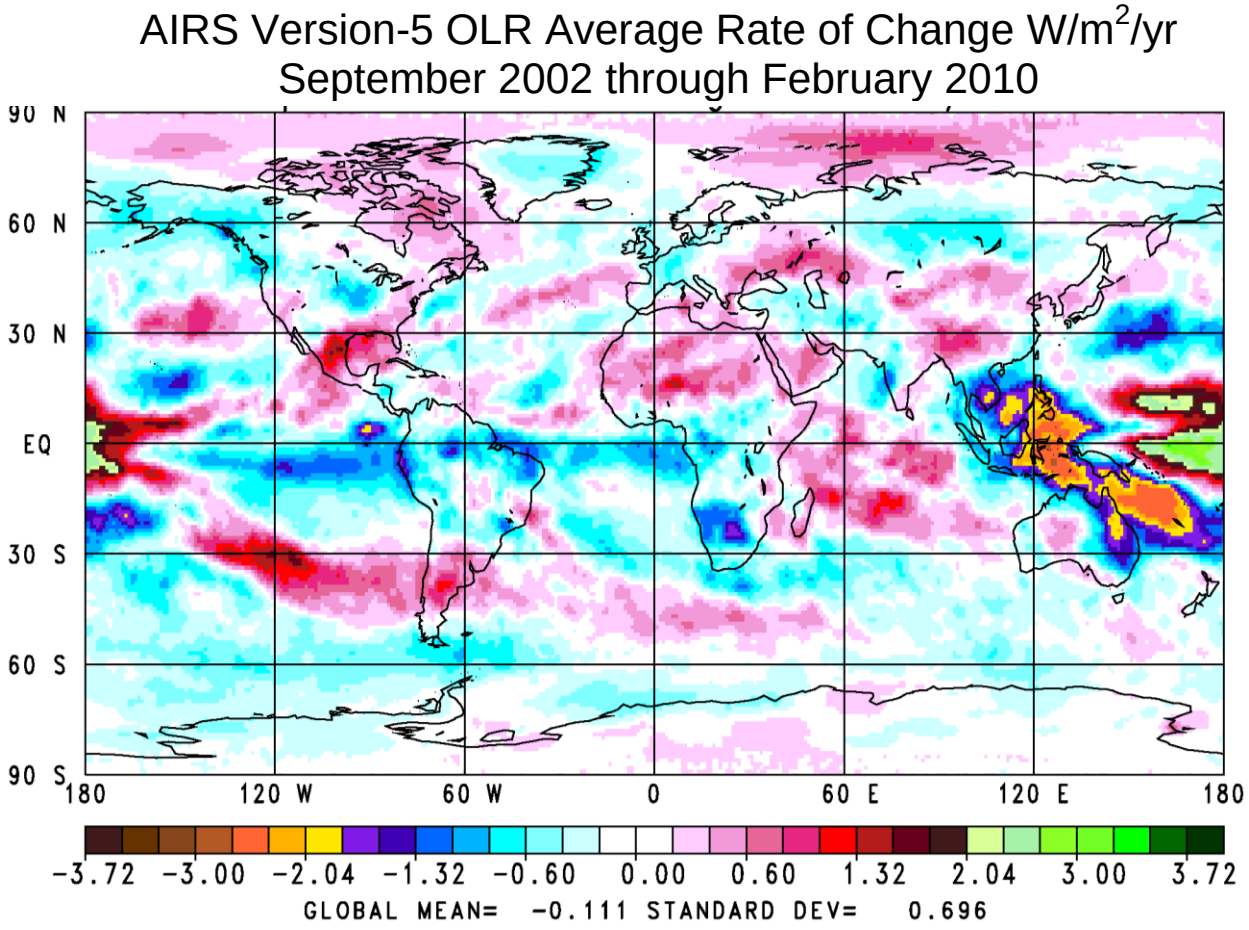

Figure 7a. Spatial 1° latitude by 1° longitude distributions of Global OLR ARC's over the time period September 2002 through February 2010. Figure 7a shows the ARC for AIRS Version-5.

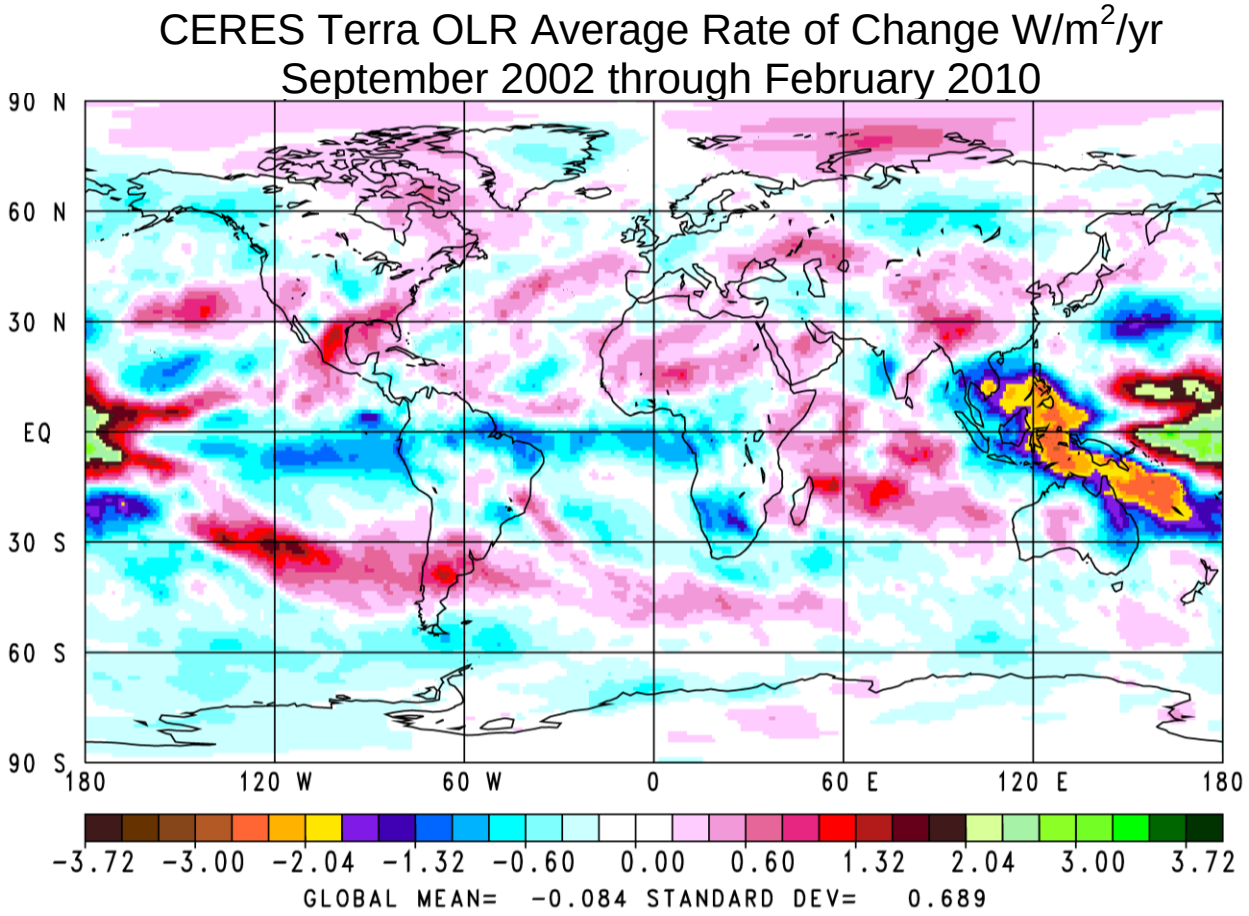

Figure 7b. Shows the ARC for CERES Terra Edition-2.5.

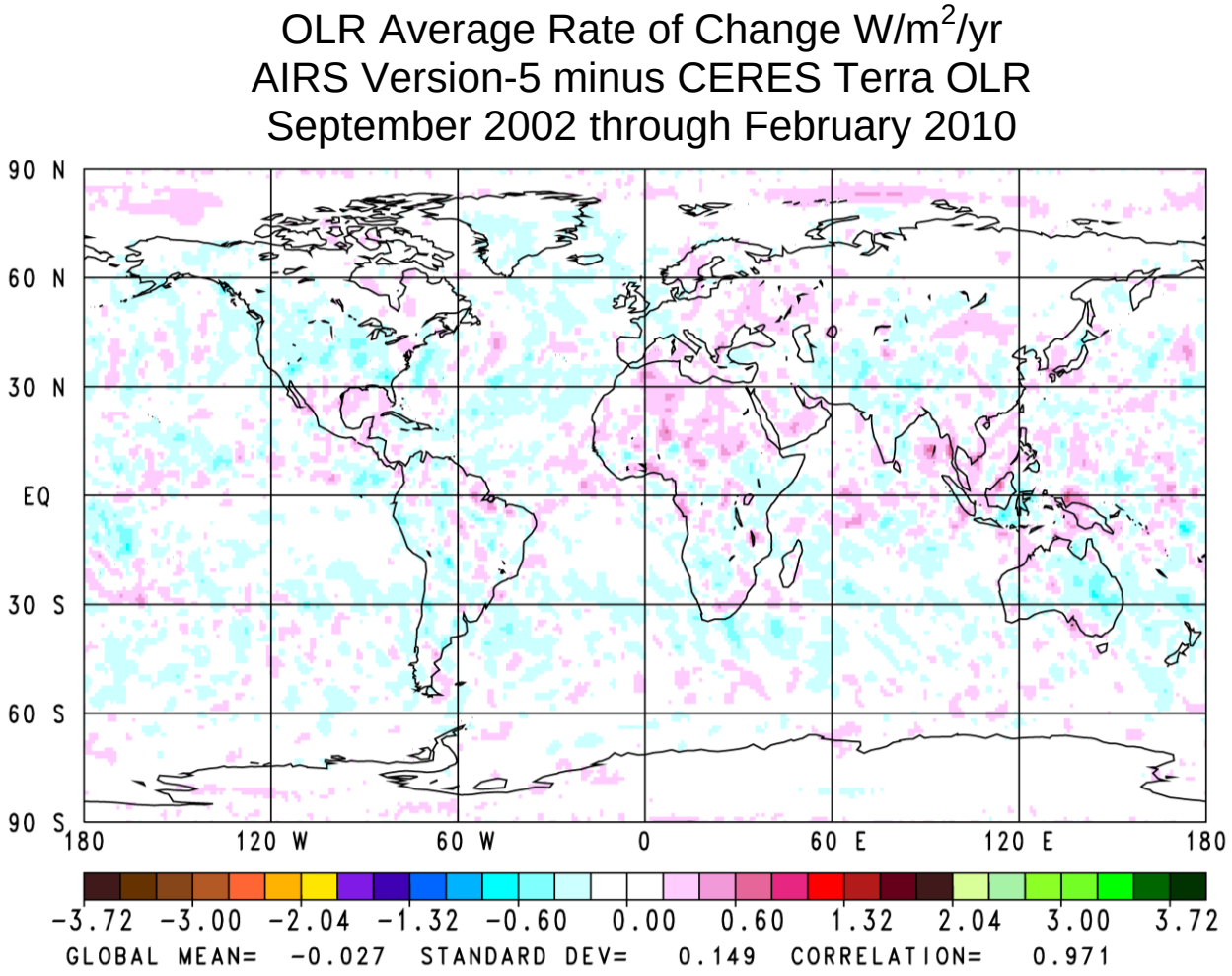

Figure 7c. Shows the ARC difference between AIRS Version-5 and CERES Terra Edition-2.5.

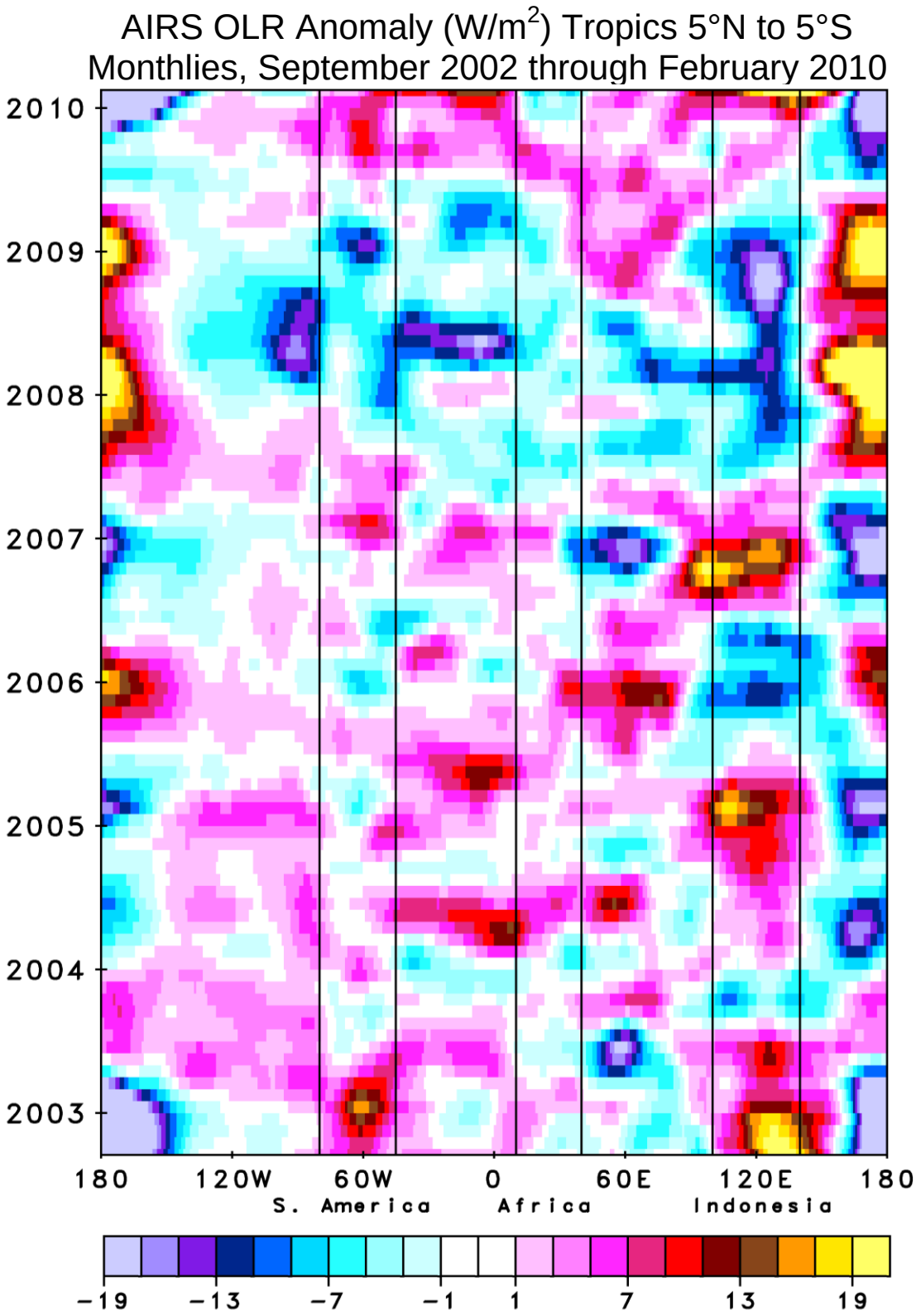

Figure 8a Hovmöller diagrams for time series of monthly mean OLR anomalies integrated over the latitude range 5°N through 5°S, in each 1° longitude bin for the period September 2002 through February 2010. Figure 8a shows the OLR anomalies for AIRS Version-5.

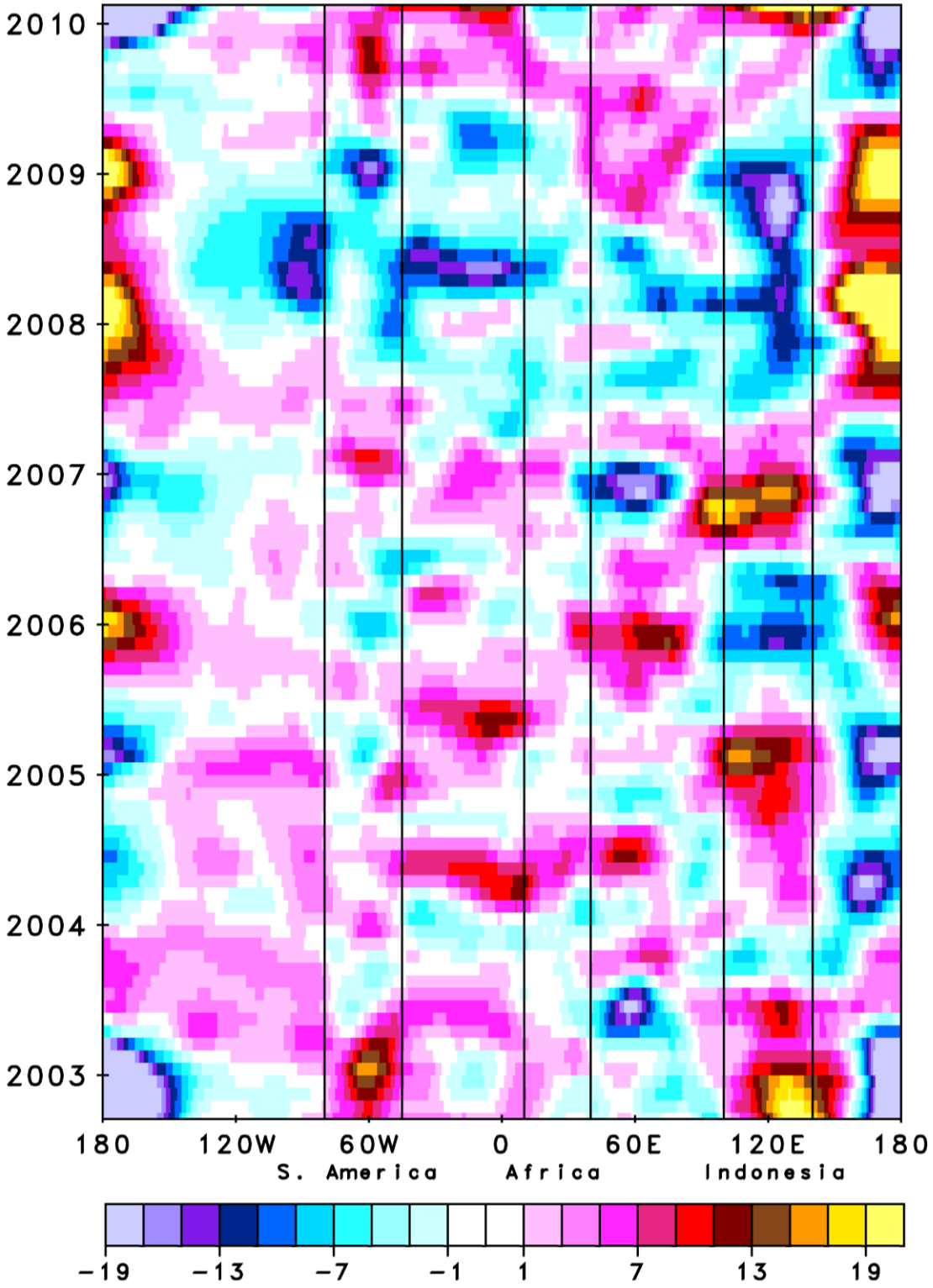

Figure 8b. Shows the OLR anomalies for CERES Terra Edition-2.5.

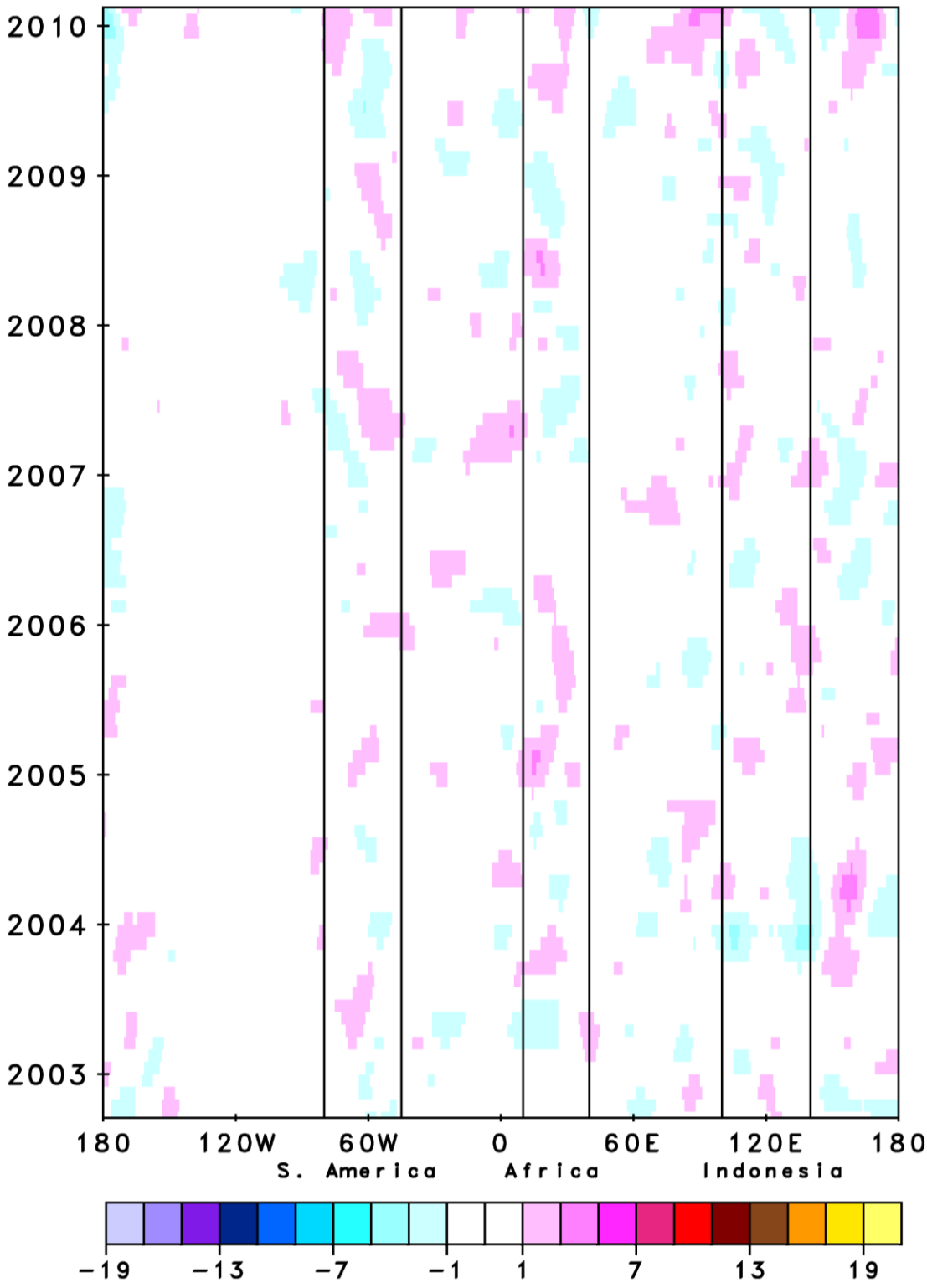

Figure 8c. Shows the OLR anomalies difference between AIRS Version-5 and CERES Terra Edition-2.5.

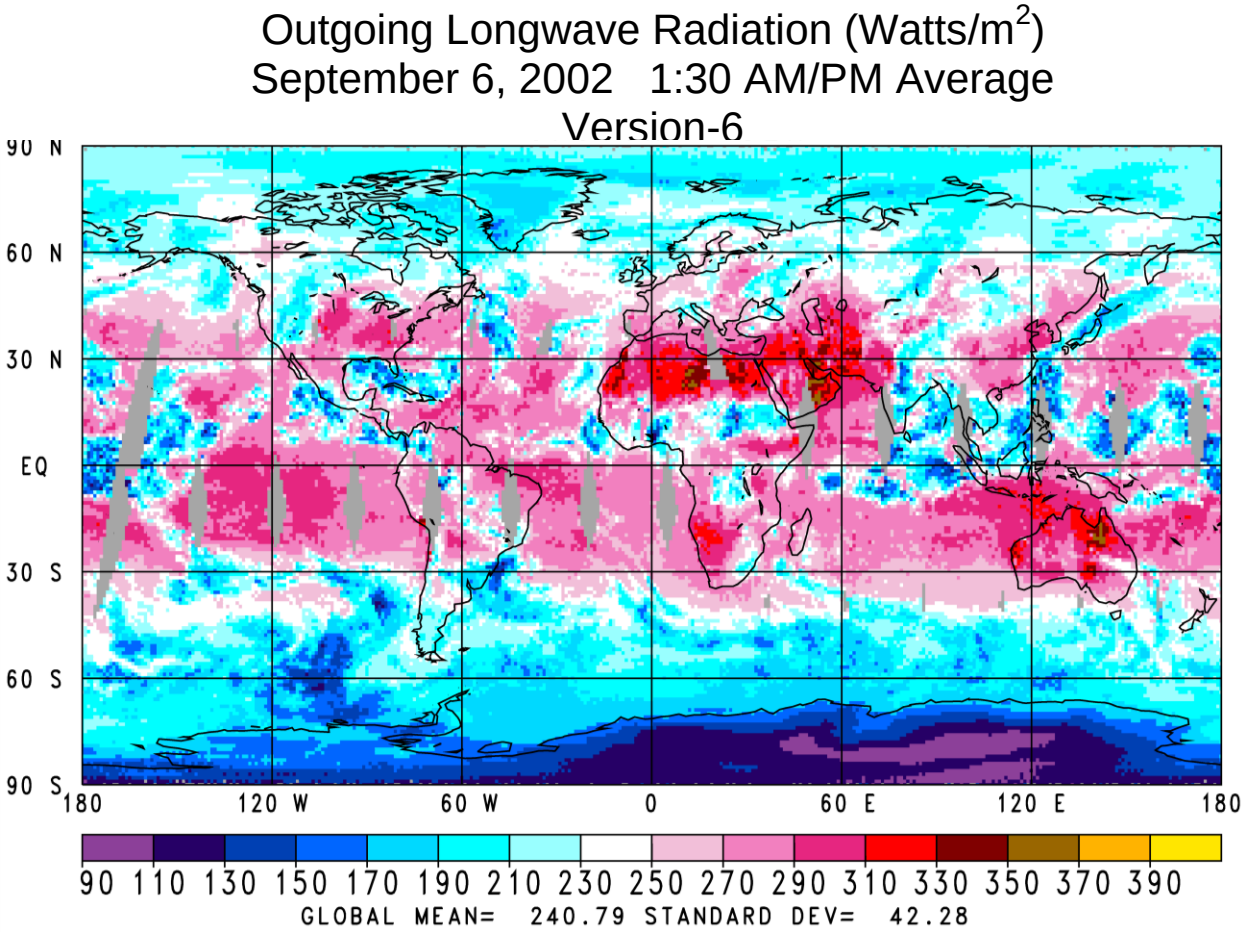

Figure A1a. The spatial distribution of 1:30 AM/PM average OLR computed for September 6, 2002 using the current version of the AIRS Science Team Version-6 retrieval algorithm.

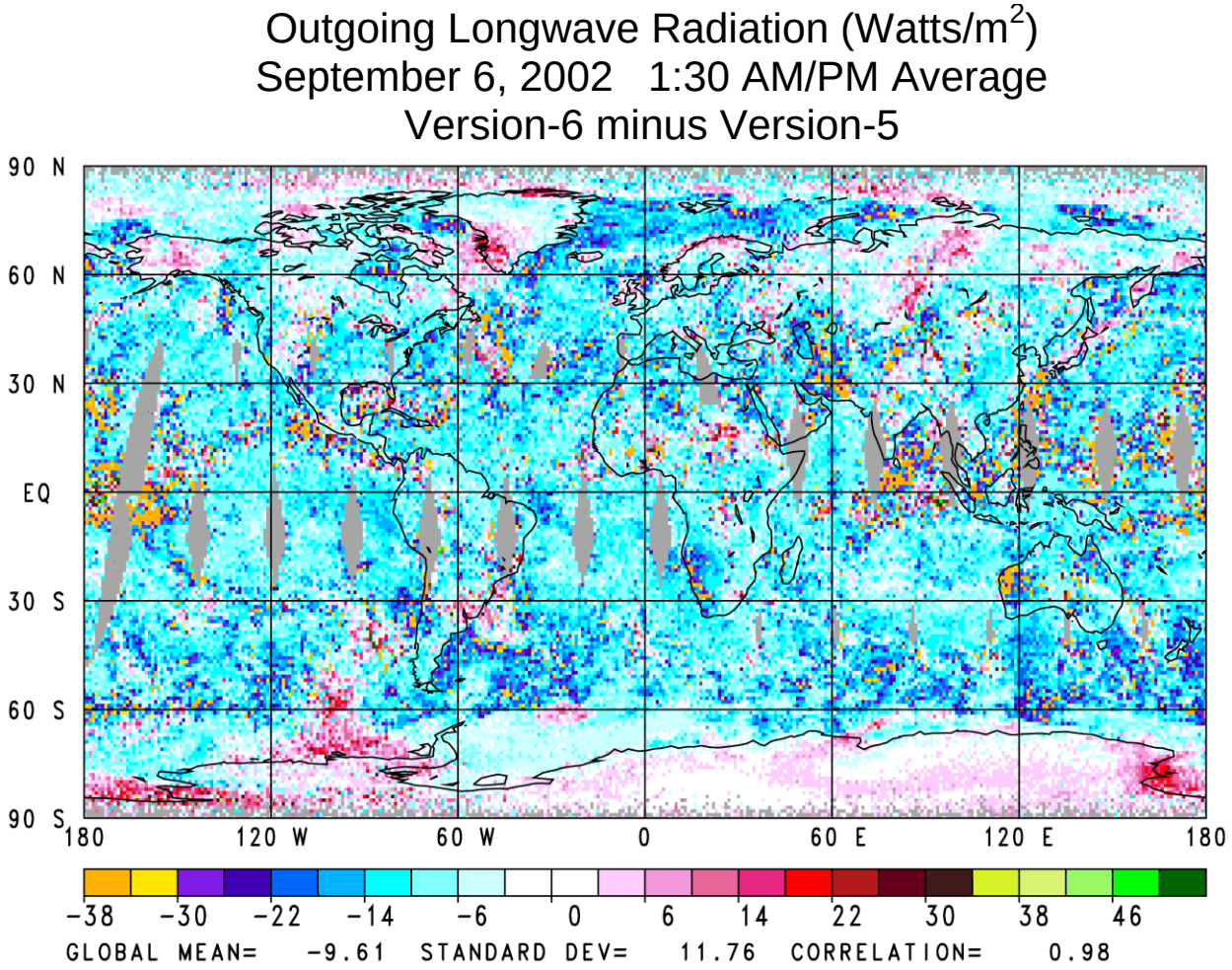

Figure A1b. The AIRS Science Team Version-6 OLR minus Version-5 OLR for 1:30 AM/PM average of September 6, 2002.

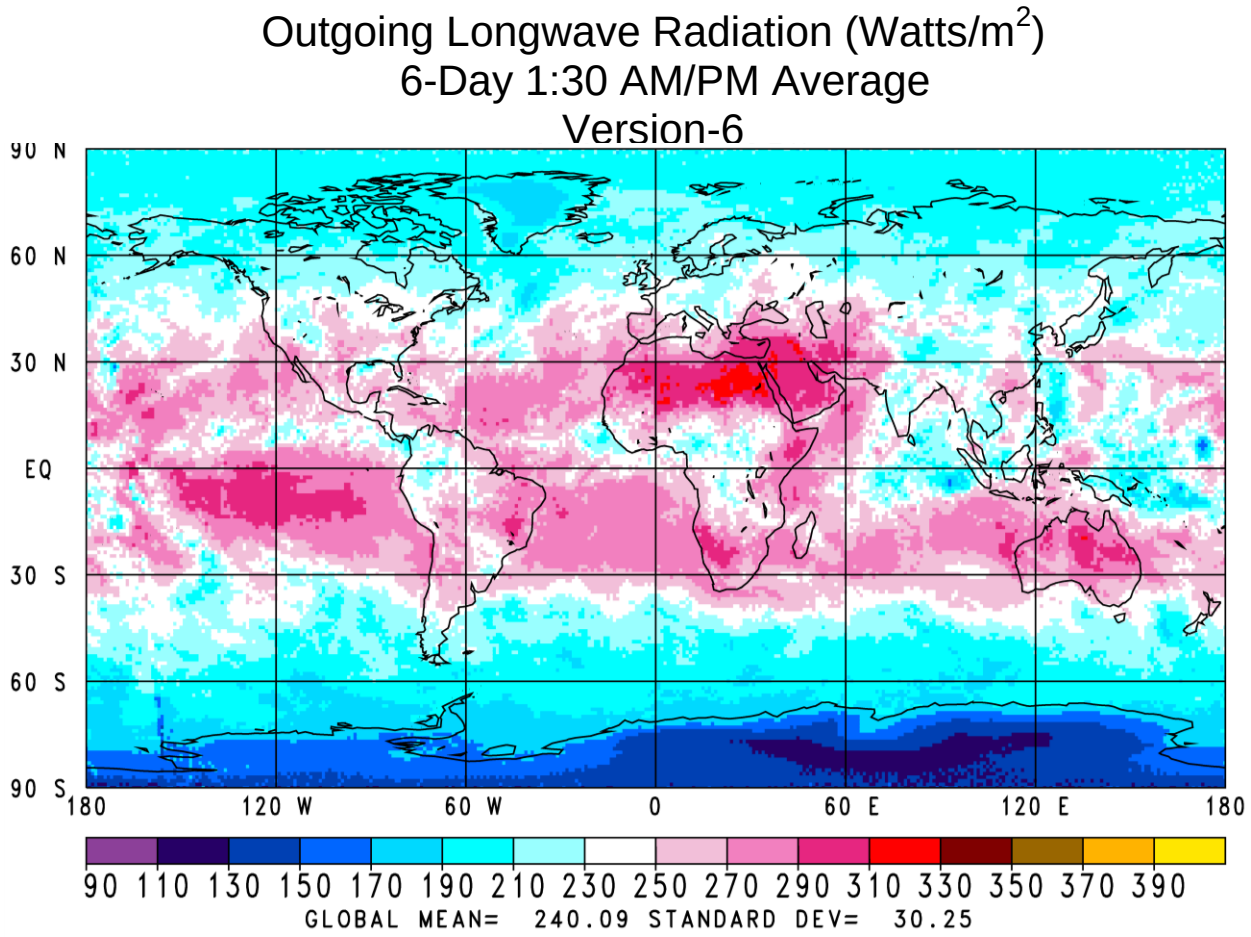

Figure A2a. The AIRS Science Team Version-6 OLR for 1:30 AM/PM average of September 6, 2002, January 25, 2003, September 29, 2004, August 5, 2005, February 24, 2007, and August 10, 2007.

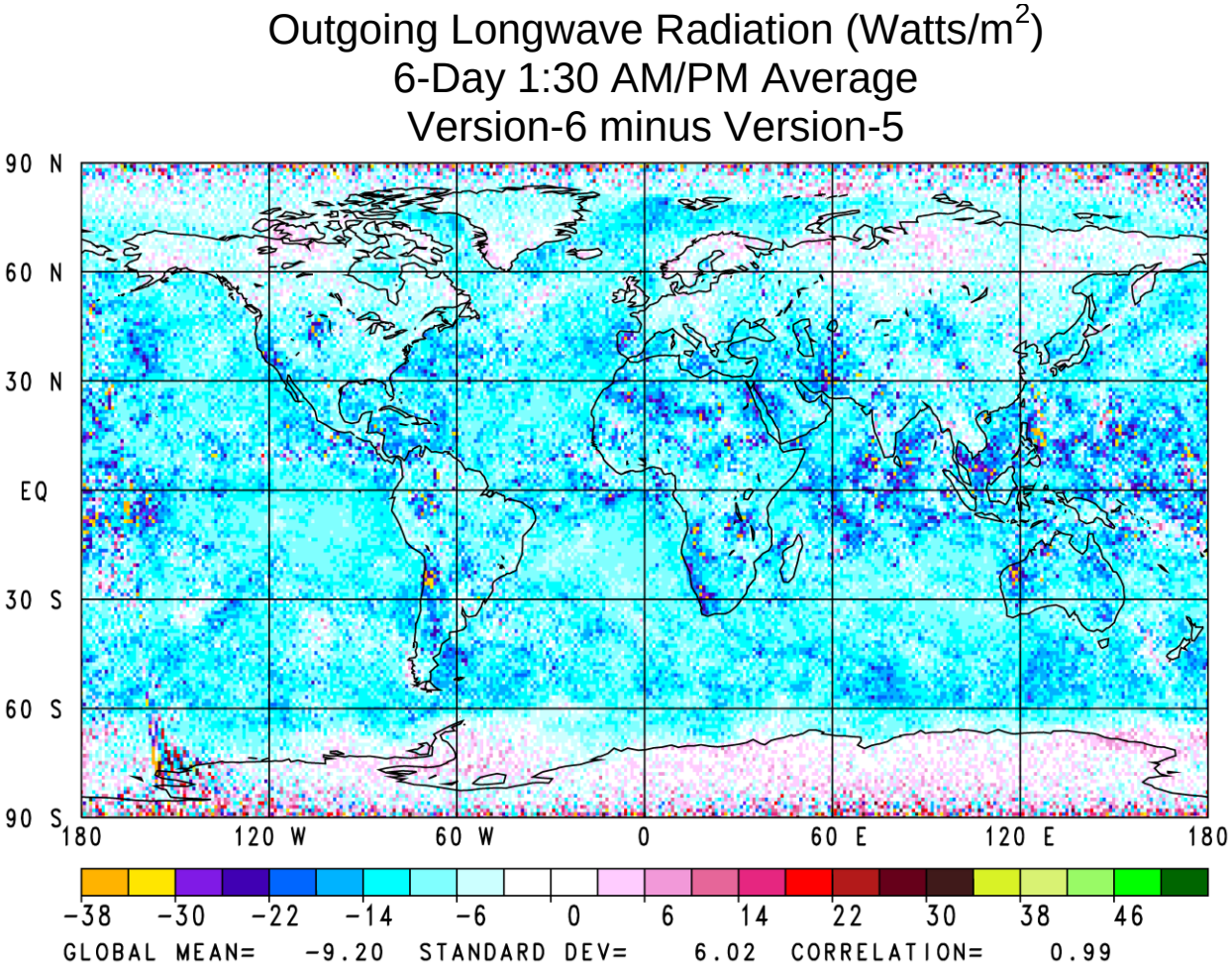

Figure A2b. The AIRS Science Team Version-6 OLR minus Version-5 OLR for the 1:30 AM/PM average of the six day period.